

PAPER • OPEN ACCESS

An investigation of the chill-casting interface dynamics in production of sand-cast A319 engine blocks

To cite this article: Farzaneh Farhang Mehr *et al* 2019 *IOP Conf. Ser.: Mater. Sci. Eng.* **529** 012080

View the [article online](#) for updates and enhancements.



IOP | ebooks™

Bringing you innovative digital publishing with leading voices to create your essential collection of books in STEM research.

Start exploring the collection - download the first chapter of every title for free.

An investigation of the chill-casting interface dynamics in production of sand-cast A319 engine blocks

Farzaneh Farhang Mehr¹, Steve Cockcroft¹ and Daan Maijer¹

¹Materials Engineering Department, The University of British Columbia, 309, 6350 Stores Road, Vancouver, BC, Canada, V6T 1Z4

farzaneh.fmehr@ubc.ca

Abstract. In recent years, the automotive industry has been increasing the production of small, high-power gas engines as part of several strategies to achieve the new “Corporate Average Fuel Economy” (CAFE) standards. This trend requires an improvement in the thermal and mechanical fatigue durability of the aluminium alloys used in the production of the cylinder blocks in these engines. Conventionally, solid chills are employed in areas of these castings subject to high cyclic loading to enhance the mechanical performance of the cast material – i.e. in the main bearing bulkhead. A potential means of improving the efficacy of these chills is to incorporate water cooling. To assess the effectiveness of this method, a water-cooled chill was designed and installed in a bonded-sand engine block mould package (1/4 section). The moulds were instrumented with thermocouples, to measure the evolution of temperature at key locations in the casting, and “Linear Variable Displacement Transducers” (LVDTs), to measure the gap formation at the interface between the chill and the casting. This paper summarizes, at a high level, some of the findings of this work.

1. Introduction

The automotive industry is working to meet the stricter efficiency requirements laid out within the CAFE (Corporate Average Fuel Economy) regulations [1], while at the same time not sacrificing performance. One approach is to increase the use of lightweight materials, which leads to a decrease in the overall vehicle weight and fuel consumption [2,3]. Other approaches include smaller displacement engines and gas-electric hybrid drivetrains. However, one trend that is becoming clear, is a greater emphasis on force induction gasoline engines. This allows for weight reduction to be achieved with smaller displacement engines without sacrificing performance. One consequence of this approach is that the engine block materials are subject to higher in-service thermal and mechanical cyclic loads [3,4].

The fatigue properties of an alloy are strongly affected by a number of the as-cast microstructure features including, Secondary Dendrite Arm Spacing (SDAS), porosity and eutectic lamella spacing (including intermetallic β -Al₅FeSi platelets) [5-7]. It is generally accepted these features can act as fatigue initiation sites and that a reduction in their size will result in an improvement in fatigue performance. For a given alloy chemistry, one of the key parameters affecting the length scale of all three is cooling rate [8].

Engine blocks and cylinder heads include thick and thin sections, at different distances from the gating system. In the absence of chills, the thick sections will undergo slower cooling rates during



solidification, have coarser microstructures, and will exhibit relatively poorer fatigue properties than thinner, more rapidly solidified sections. By design, the thicker sections also correspond with highly stressed areas, such as for example the engine block main bearing bulkheads. Hence, particular attention needs to be applied to these areas to achieve suitable in-service performance. The application of a well-designed metallic chill, which is directly in contact with the solidifying metal, can increase the heat flow from the thick sections resulting in a finer microstructure and better fatigue performance. Typically, solid H13 tool steel chills are used for this purpose in the precision sand casting industry. Often they are preheated, to avoid formation of a columnar structure directly adjacent to the chill. However, this approach limits the capacity of the chill to refine the structure deep into the bulkhead, which is needed for the high-power density engines.

This paper presents some of the preliminary results obtained with a water-cooled H13 chill using a casting geometry based on a section of an engine block including the main bearing bulk head and a cylinder. The cooling strategy explored is to initially achieve a low cooling rate directly adjacent to the chill, to avoid a columnar structure and cold shuts, and then to achieve a high, sustained, cooling rate to reduce the microstructural length scales deep into the casting, thereby improving component fatigue performance.

2. Experimental

The sand moulds used in these experiments were one-quarter sections of a 2.0 liter turbocharged 4-cylinder engine block mould package, designed at General Motors Co. to approximate the cooling conditions in a production engine block for experimental and research purposes. Figure 1 shows a side view of the assembled mould package with the refractory board removed from the face oriented toward the camera (the light blue refractory board can be seen fixed to the back of the of the other side). The solid version of the H13 chill can be seen sitting on top of the mould cavity, directly above the main bearing bulk head. Figure 2 shows the casting including the feeding system following cooling and extraction from the sand mould.



Figure 1. Mould package for a section of a 2.0 liter turbocharged 4-cylinder engine block



Figure 2. Cast engine block section – the lines show the approximate locations where metallography samples were taken

Figure 3 shows the geometries of the solid chill and the water-cooled chill fabricated at UBC for this investigation. The water-cooled chill was designed based on preliminary experimental and modelling results as a part of this research at UBC. Both chills were made of H13 tool steel.

Prior to casting, eleven Type-K thermocouples, 0.5 mm diameter wire, sheathed in a nickel–chrome-based alloy (10mm Super OMEGACLAD XL), were installed in the mould package at various locations including in the mould cavity – see Figure 4, which shows the post-cast location of the thermocouples.

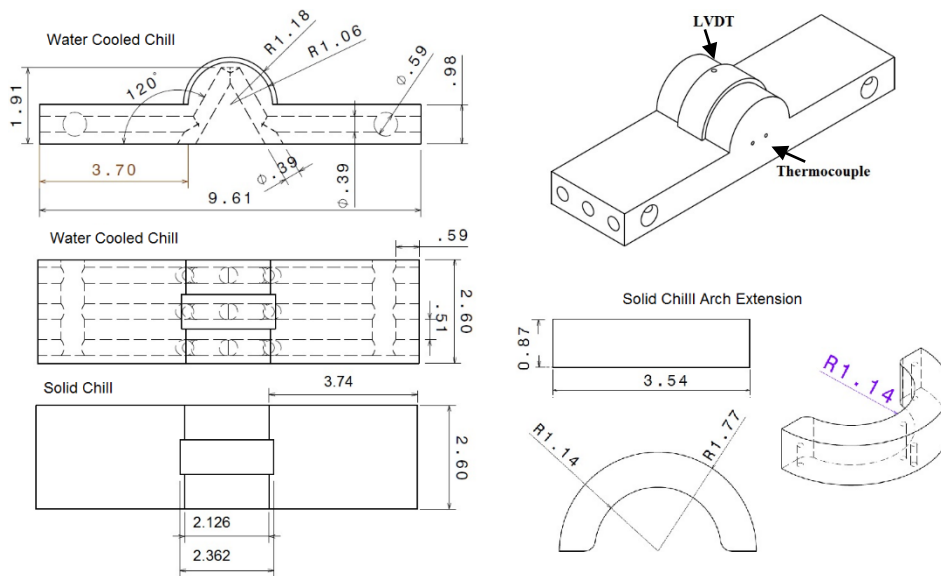


Figure 3. Configuration of the water-cooled chill, the solid chill, and the solid chill arch extension

The thermocouple wires were exposed at the tip and twisted to form the thermocouple junction. A total of two thermocouples were inserted in the bulkhead area at 10 and 30 mm away from the chill, underneath the flat section of the chill. Also, three thermocouples were inserted in the cylinder area at 10, 60, and 110 mm from the bulkhead, and four thermocouples were inserted in the cylinder water jacket area (Casting TC6-TC9). All these thermocouples were placed at the centre of the mould cavity. These measurements enabled the investigation of the variation in cooling rate with distance from the chill. Further, in order to monitor the evolution of temperature in the chill, two thermocouples (also Type-K, sheathed in alumina tubes) were placed in the middle of the chill, in the arch section – see Figures 3 and 4.

The evolution in the displacement of the casting and chill at the casting/chill interface was measured by using two LVDTs (Schaevitz –HR 050), one placed in contact with the chill and the other passing through the chill, and protruding about 2mm into the mould cavity (Figure 3). Both LVDTs were also equipped with a thermocouple (Type K, sheathed in alumina tubes) to record the temperature at both sides of the interface. The temperature-time data for the in-mould thermocouples, in-chill thermocouples and the displacement data from the two LVDTs were recorded at a frequency of 5Hz, with the use of “Lab View” software.

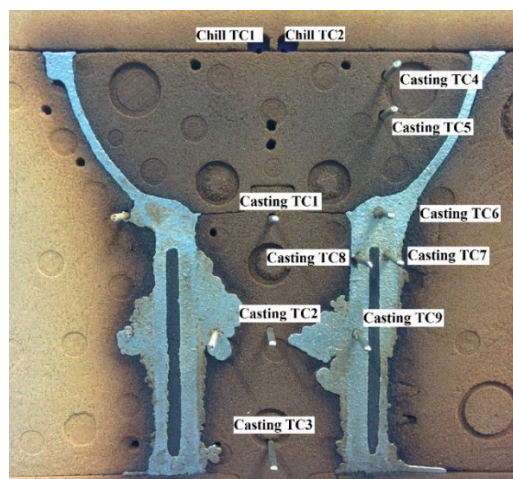


Figure 4. Thermocouple Locations in the Casting and the Chill

In this research, A319 aluminium alloy was used, which is a widely used alloy for the commercial production of engine blocks and cylinder heads in North America. The alloy composition is presented in Table 1. The pouring process started when the temperature of molten metal was $750\pm 5^\circ\text{C}$. For the water-cooled chill, the water was switched on 10 seconds after the completion of pouring process and the water flow rate was set to $35\text{ L}\cdot\text{min}^{-1}$ (measured with an inline water flow meter). The temperature of the main water supply was fairly constant at $\sim 10^\circ\text{C}$.

Table 1. Chemical Composition of A319 Alloy

Alloying Element	Si	Fe	Cu	Mn	Mg	Zn	Ti	Sr	Al
Balance (wt%)	8.10- 8.75	0.27- 0.59	2.60- 2.95	0.19- 0.44	0.31- 0.4	0.4- 0.8	0.12- 0.16	0.004 max	Bal.

In order to investigate the effect of variation in cooling rate on the SDAS, thirty $10\times 10\times 5$ mm metallographic specimens were taken at 5, 10, 15, 20, and 25 mm from the chill at three angular locations on the arch: 1) along a line normal to the tangent at 45° to the top surface of the chill; 2) along a line normal to the tangent at 90° ; and 3) along a line normal to the tangent at 135° - see Figure 2. The metallographic samples were polished down to $0.1\mu\text{m}$ and etched using 0.5% HF solution. Metallographic images were taken with a Nikon Epiphot 300 optical microscope, equipped with a QImaging digital camera. The SDAS was estimated in each sample (100 measurements per sample) using the line intercept procedure and was taken as a representative measurement of the microstructure length scale.

3. Results and Discussion

Figure 5 shows selected thermocouple data for both the water-cooled and solid chill castings from 4 different regions of the engine block - the casting/chill interface, the bulkhead area (Casting TC5), the cylinder barrel area (Casting TC1) and cylinder water-jacket area (Casting TC6) - see also Figure 4. The solidus and liquidus lines have also been added to the plots to aid with identifying the solidification temperature range. It can be observed that the water-cooled chill does not significantly alter the solidification time relative to the solid chill in the cylinder barrel (TC1) and the water-jacket areas (TC6), as would be expected. These areas are far away from the chill and will only be affected at longer times, as shown. However, at the casting/chill interface and 30mm away from the chill in the bulk head (TC5) there is a significant effect. The cooling curves for the water-cooled chill reach a lower measured peak and show a substantially higher cooling rate, compared to the data from the solid chill. Three cooling curves show that the peak measured temperature falls below the solidus temperature. The reason for this behaviour is unclear and may be related to a combination of the loss of superheat in the metal by the time it reaches the top of the bulk and slow response time of the thermocouple, albeit the TC5 temperature data for solid chill does not show this problem.

A comparison between the thermocouple data extracted from the chills - water-cooled and solid - is shown in Figure 6. The solid chill temperature at 2mm from the interface rapidly increases to approximately 250°C in the first 50 seconds, then levels off followed by a slight increase to $\sim 300^\circ\text{C}$ up to 800 seconds, when it becomes thermally saturated. The other two thermocouples farther from the interface in the solid chill (TC1 and 2) show a less rapid initial increase in temperature to $\sim 180^\circ\text{C}$ during the first 200 seconds, followed by a marginal increase to $\sim 260^\circ\text{C}$ at 800 seconds. In contrast, in the water-cooled chill, there is an initial increase in temperature to a maximum of $\sim 290^\circ\text{C}$ at the chill/casting interface (2mm from the interface) in the period when the water cooling is off. At the onset of water cooling, the temperature drops to $\sim 75^\circ\text{C}$ and then rebounds to 150°C prior to slowly declining. It is unclear what is responsible for the rebound in temperature.

These results indicate that water-cooling has the potential to greatly increase the thermal extraction capacity of the chill. Hence, water-cooling may be an effective method for maintaining a large

temperature difference between the chill and the casting– i.e. sustaining a large driving force for heat transfer at the casting/chill interface and enhancing heat transport.

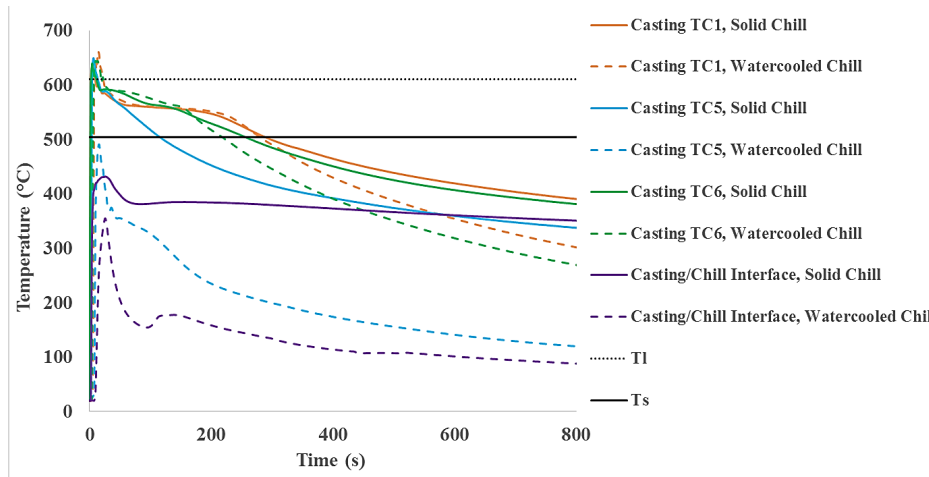


Figure 5. Comparison between thermocouple data from the casting chill interface, bulkhead (Casting TC5), cylinder barrel (Casting TC1) and water jacket (Casting TC6) for the water-cooled and solid chill castings

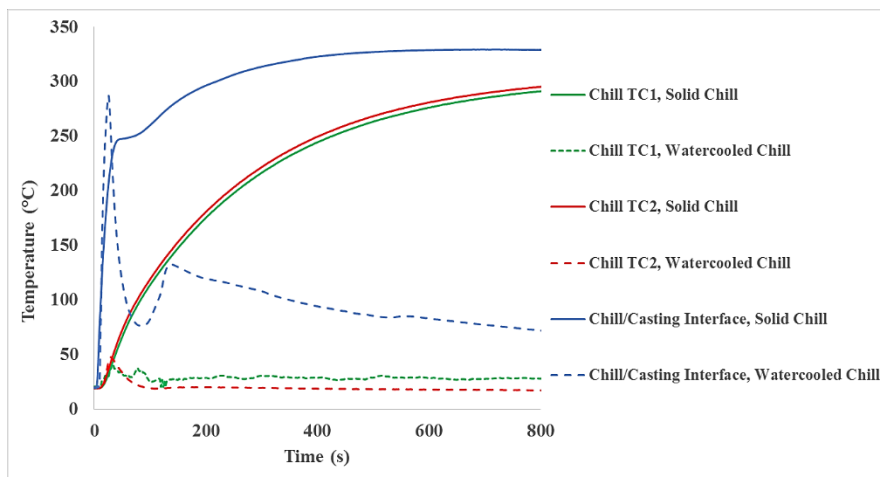


Figure 6. Comparison between thermocouple data for the Chill/Casting Interface, Chill TC1 and Chill TC2 for the water-cooled chill and the solid chill.

Figure 7 shows a comparison between the evolution in the casting/chill interface gap in the two castings - water-cooled and solid chill. The results suggest that the interface gap is about 10 times larger in the solid chill casting. Consequently, the resistance to heat transfer at the casting/chill would be larger in the case of solid chill casting further reducing the efficacy of the chill. The reason for the difference in gap formation is still under investigation and may be related to the expansion of the arch forcing the chill upward.

Figure 8 shows a comparison between SDAS in the two castings. In each casting, the SDAS increases with increasing distance from the chill – i.e. decrease in the cooling rate – as would be expected. Also, the measurements suggest that SDAS in water-cooled chill samples were approximately 20% smaller than SDAS in the solid chill samples. This result supports the fact that employing the water-cooling can increase the solidification rate and as a result, refine the microstructure of the casting, which should lead to an improvement in mechanical fatigue properties of the cast component.

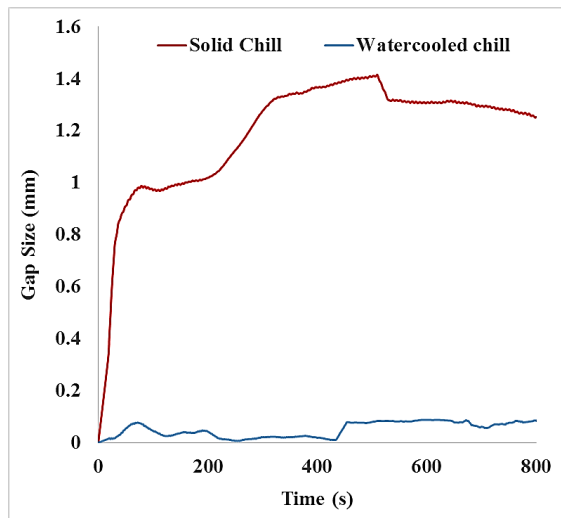


Figure 7. Comparison between the casting/chill interface gap in the water-cooled chill and the solid chill castings.

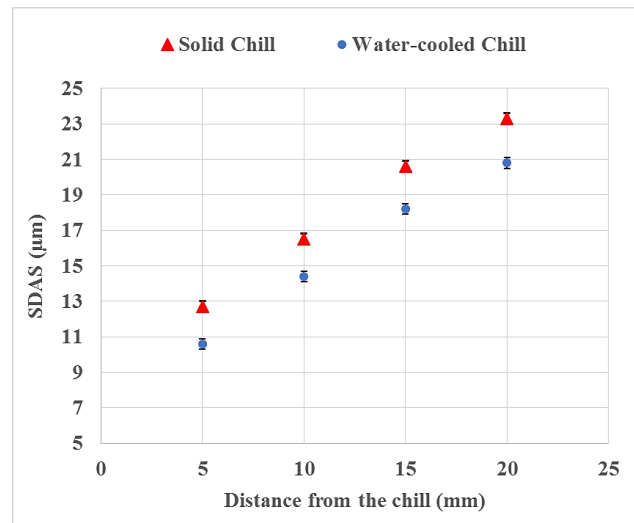


Figure 8. Comparison between the SDAS Size in the water-cooled chill and solid chill castings (the error bars represent the standard error)

4. Summary and Conclusion

The present work involved conducting a series of experiments to determine the efficacy of a water-cooled chill in refining the microstructure of a 2.0 liter turbocharged, 4-cylinder engine block, in the bulkhead section. For this purpose, a section of an engine block was cast employing both a solid H13 chill and a water-cooled H13 chill. The results show that using the water-cooled chill was effective in increasing the cooling rate in the bulkhead and reducing the SDAS and therefore has the potential to improve the mechanical properties in the highly stressed bulkhead region of the cylinder block. The main conclusions from this work are:

1. Using the water-cooled chill was found to be effective in decreasing the cooling rate in the bulkhead area of the engine block section.
2. A 20% reduction in the SDAS size in the bulkhead area of the engine block was achieved by using the water-cooled chill.
3. The solid chill was found to generate a larger interfacial gap than the water-cooled chill.

Further experimental and modeling work is needed in order to characterize the casting/chill interface heat transfer behavior in both the solid chill casting and the water-cooled chill casting.

Acknowledgement

The authors would like to acknowledge General Motors Co., and in particular, Mike Walker for providing the sand moulds.

References

- [1] Bastani, P., Heywood, J., Hope, C. (2012). *MIT Energy Initiative Report*.
- [2] Mackay, R., Byczynski, G. (2011). *Shape Castings: The 4th International Symposium in Honor of Prof. John T Berry*, 191-198.
- [3] Miller, W., Zhuang, L., Bottema, J., Wittebrood, A., De Smet, P., Haszler, A., & Vieregge, A. (2000). *Materials Science and Engineering A*, 280, 37-49.
- [4] Heysler, L., Feikus, F., & Otte, M. (2001). *AFS Transactions*, 50, 1-9.
- [5] Mackay, R., & Szablewski, D. (2010). *International Journal of Metalcasting*, 4, 31-45.
- [6] Mackay, R., & Sokolowski, J. (2010). *International Journal of Metalcasting*, 4, 33-50.
- [7] Viet-Duc, L., Morel, F., Bellett, D., Pessard, E., Saintier, N., & Osmond, P. (2015). *Procedia Engineering*, 133, 562-575.
- [8] Mackay, R., Djurdjevic, M., & Sokolowski, J. (2000). *AFS Transactions*, 25, 521-530.